ELSEVIER

Journal of Biomechanics 41 (2008) 1015–1021

JOURNAL OF BIOMECHANICS

www.elsevier.com/locate/jbiomech
www.JBiomech.com

A model of growth and rupture of abdominal aortic aneurysm

K.Y. Volokh[a,*], D.A. Vorp[b]

[a]*Faculty of Civil and Environmental Engineering, Technion—I.I.T., Haifa 32000, Israel*
[b]*Departments of Surgery and Bioengineering, Center for Vascular Remodeling and Regeneration, University of Pittsburgh, PA 15213, USA*

Accepted 12 December 2007

Abstract

We present here a coupled mathematical model of growth and failure of the abdominal aortic aneurysm (AAA). The failure portion of the model is based on the constitutive theory of softening hyperelasticity where the classical hyperelastic law is enhanced with a new constant indicating the maximum energy that an infinitesimal material volume can accumulate without failure. The new constant controls material failure and it can be interpreted as the average energy of molecular bonds from the microstructural standpoint. The constitutive model is compared to the data from uniaxial tension tests providing an excellent fit to the experiment. The AAA failure model is coupled with a phenomenological theory of soft tissue growth. The unified theory includes both momentum and mass balance laws coupled with the help of the constitutive equations. The microstructural alterations in the production of elastin and remodeling of collagen are reflected in the changing macroscopic parameters characterizing tissue stiffness, strength and density. The coupled theory is used to simulate growth and rupture of an idealized spherical AAA. The results of the simulation showing possible AAA ruptures in growth are reasonable qualitatively while the quantitative calibration of the model will require further clinical observations and in vitro tests. The presented model is the first where growth and rupture are coupled.

Keywords: Abdominal aortic aneurysm; Growth; Rupture; Model; Failure; Softening; Hyperelasticity

1. Introduction

The condition of a focal dilation of the infrarenal aorta—abdominal aortic aneurysm (AAA)—is found in $\approx 2\%$ of the elderly population, with $\approx 150{,}000$ new cases diagnosed each year, and the occurrence is increasing (Bengtsson et al., 1996; Ouriel et al., 1992). In many cases AAA gradually expands until rupture causing a mortality rate of 90%. The AAA rupture is considered the 13th most common case of death in the US (Patel et al., 1995). Since the AAA treatment is expensive and bears considerable morbidity and mortality risks it is vital to predict when the risk of rupture justifies repair. Such a prediction should be based on a biomechanical model of growth and rupture of the aneurysm.

Very few models of aneurysmal growth have been developed: Humphrey and Canham (2000); Watton et al. (2004); Baek et al. (2006); and some empirical criteria of the aneurysm rupture were proposed: Elger et al. (1996); Li and Kleinstreuer (2005). Though the models incorporate growth descriptions, none of them couples growth with rupture in the theoretical setting. The latter is important in order to provide an objective criterion of the material failure, which is a part of the model formulation and not an external condition imposed on the stress/strain field. Besides, the insertion of the failure description makes the model more physical because no real material can sustain large enough strains—it should fail. Existing models of soft tissues including AAA do not describe failure. According to the traditional models, the material is always intact independently of the amount of the accumulated energy or strain. The latter is unphysical, of course. The coupling of growth and rupture is the primary goal of the present work.

Our description of rupture is based on the idea that a small (infinitesimal) material volume possesses a limited capacity of accumulating energy under increasing strain.

*Corresponding author. Tel.: +972 48292426; fax: +972 48295697.
E-mail address: cvolokh@tx.technion.ac.il (K.Y. Volokh).

0021-9290/$ - see front matter © 2007 Elsevier Ltd. All rights reserved.
doi:10.1016/j.jbiomech.2007.12.014

Volokh (2007) shows that the average energy of the atomic/molecular bonds sets the failure energy limit, which is a material constant. This new failure constant controls softening in the constitutive law. An application of the average bond energy to analysis of the overall strength of an intact arterial wall can be found in Volokh (2008). In the present work, we introduce the AAA model in the form of isotropic and incompressible Neo-Hookean type material with softening. All material constants are calibrated in the uniaxial tension (UT) test for an AAA sample. The calibrated rupture model is further enhanced with a description of growth (Volokh, 2004, 2006b), which incorporates the law of mass balance/evolution with a source term related with the tissue remodeling and an additional term in the stored energy expression related with the material expansion under the mass supply. The proposed coupled model is used to simulate the evolution and rupture of an idealized spherical AAA. The results of the simulation encourage further development and calibration of the model, concerning growth, when more data is collected.

2. AAA rupture model

2.1. AAA model with softening

We consider the classical formulation of nonlinear elasticity according to which a generic material particle of body Ω occupying position $\mathbf{X}$ in the reference configuration moves to position $\mathbf{x}(\mathbf{X})$ in the current configuration. The deformation of the particle is defined by the tensor of deformation gradient, $\mathbf{F}=\partial\mathbf{x}/\partial\mathbf{X}$. The equilibrium equation, $\mathrm{div}\,\boldsymbol{\sigma}=\mathbf{0}$ in Ω, and boundary conditions $\mathbf{x}=\bar{\mathbf{x}}$ on $\partial\Omega_{\mathbf{x}}$ or $\boldsymbol{\sigma}\mathbf{n}=\bar{\mathbf{t}}$ on $\partial\Omega_{\mathbf{t}}$, should be obeyed, where 'div' operator is with respect to the current position, $\mathbf{x}$; $\boldsymbol{\sigma}$ is the Cauchy stress tensor; $\mathbf{t}$ is the traction per unit area of the current surface with the unit outward normal $\mathbf{n}$; and the barred quantities are prescribed.

We assume that the material is incompressible, $\det\mathbf{F}=1$. Such an assumption is often used for analysis of soft biological tissue because its response to hydrostatic pressure is much stronger than to shearing. It seems, however, that the applicability of the incompressibility assumption essentially depends on the specific loading and deformation of the material under consideration (Volokh, 2006a).

We further assume that the material is hyperelastic and can be described by a stored energy function. Traditionally, the stored energy of hyperelastic materials is defined as $\psi=W$, where W is used for the strain energy of the *intact* material, i.e. the material that does not undergo failure. Such a material is characterized as follows: $||\mathbf{C}||\to\infty\Rightarrow\psi=W\to\infty$, where $||\ldots||$ is a tensorial norm and $\mathbf{C}=\mathbf{F}^{\mathrm{T}}\mathbf{F}$ is the right Cauchy–Green deformation tensor. Simply speaking, an increasing strain increases the accumulated energy unlimitedly. Evidently, the consideration of materials that do not undergo failure is restrictive and no real material can sustain large enough strains. The energy increase of a real material should be limited, $||\mathbf{C}||\to\infty\Rightarrow\psi\to\phi=\text{constant}$, where ϕ can be called the *material failure energy*. Among a variety of possibilities to formulate the strain energy obeying this condition our desire is to enrich the already existing models, which describe intact behavior of materials reasonably well, with the failure condition. Such a desire can be formalized as follows: $||\mathbf{C}||\to\infty\Rightarrow\psi(W(\mathbf{C}))\to\phi$. A *possible* solution to the problem is: $\psi(W)=\phi-\phi\exp(-W/\phi)$, where $\psi(W=0)=0$ and $\psi(W=\infty)=\phi$. In the case of the intact material behavior, $W\ll\phi$, we have $\psi(W)\approx W$ preserving the features of the intact material. The critical failure energy, ϕ, is not a purely phenomenological material constant—it has a physical meaning of the *average bond energy* and can be calculated for real materials based on the knowledge of their atomic or micro-particle structure as follows: $\phi=1/V_0\int_{V_0^*}\varepsilon D_{\mathrm{V}}\,\mathrm{d}V$, where V_0 is the reference representative volume; ε is a bond energy; D_{V} is the volumetric bond density function; and V_0^* is the integration volume defined by the range of influence of the bonds (Volokh, 2007).

Following the described approach we define the constitutive model via the following expression for the stored energy

$$\psi(I_1)=\phi-\phi\exp\left\{-\frac{\alpha}{\phi}(I_1-3)-\frac{\beta}{\phi}(I_1-3)^2\right\},\tag{1}$$

where $I_1=\mathrm{tr}\mathbf{B}=\mathrm{tr}\mathbf{C}$ is the first principal invariant of the left $\mathbf{B}=\mathbf{F}\mathbf{F}^{\mathrm{T}}$ or the right $\mathbf{C}=\mathbf{F}^{\mathrm{T}}\mathbf{F}$ Cauchy–Green deformation tensor; α and β are the elasticity constants of the material; and ϕ is an average bond energy, which is another material constant controlling its softening.

It is assumed that AAA is isotropic. The assumption is approximate, of course, because the biaxial tension tests demonstrate some deviation from it: Vorp (2007). Interestingly, the intracranial aneurysm lacks the media layer with a pronounced anisotropy while the adventitia layer has a number of sub-layers of differently oriented collagen fibers and it can also be assumed isotropic (Humphrey and Canham, 2000).

The AAA model corresponding to (1) is: $W(I_1)=\alpha(I_1-3)+\beta(I_1-3)^2$, which does not include a failure description. It was experimentally validated by Raghavan and Vorp (2000). Though the authors presented experimental data on post-failure their model was only fit to the pre-failure data.

In the present work, we use a set of the experimental data of Raghavan et al. (1996) for validation of the failure model. The data was obtained in uniaxial tests with thin strips of AAA excised from the anterior surface during surgical repair. A representative set of the data is shown with dots in Fig. 1.

Based on (1), the constitutive law for isotropic incompressible AAA tissue takes the form

$$\boldsymbol{\sigma}=-s\mathbf{1}+2\psi_1\mathbf{B},\tag{2}$$

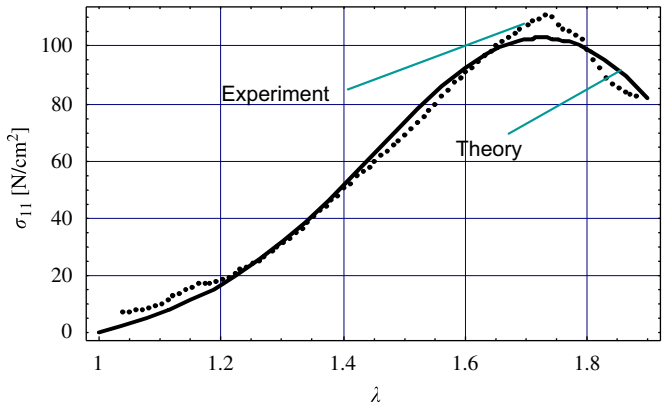

Fig. 1. Theory versus experiment for the uniaxial tension test.

where s is the Lagrange multiplier enforcing the incompressibility condition; $\mathbf{1}$ is the identity tensor and

$$\psi_1 \equiv \frac{\partial \psi}{\partial I_1} = (\alpha + 2\beta(I_1 - 3)) \exp\left\{\frac{-\alpha(I_1 - 3) - \beta(I_1 - 3)^2}{\phi}\right\}. \tag{3}$$

In the case of uniaxial tension the deformation can be described as follows

$$x_1 = \lambda X_1; \qquad x_2 = \lambda^{-1/2} X_2; \qquad x_3 = \lambda^{-1/2} X_3, \tag{4}$$

$$I_1 = \lambda^2 + \frac{2}{\lambda}, \tag{5}$$

$$\begin{aligned}\sigma_{11} &= 2(\lambda^2 - \lambda^{-1})\psi_1 \\ &= 2(\alpha + 2(I_1 - 3)\beta)(\lambda^2 - \lambda^{-1}) \\ &\quad \times \exp\left\{\frac{-\alpha(I_1 - 3) - \beta(I_1 - 3)^2}{\phi}\right\}.\end{aligned} \tag{6}$$

The theoretical curve shown in Fig. 1 has been fitted to the experimental results by minimizing the square residuals between the experimental and analytical values of stresses described by (6). The minimization procedure suggested the following best fits for the material constants: $\alpha = 10.3\,\mathrm{N/cm^2}$; $\beta = 18.0\,\mathrm{N/cm^2}$; and $\phi = 40.2\,\mathrm{N/cm^2}$.

2.2. Inflation of spherical AAA

Consider the symmetric inflation of a thin sphere in which the deformation can be presented in terms of the principal stretches as follows

$$\begin{aligned}\lambda_1 &= \lambda_2 = \tfrac{r}{R} = \lambda \\ \lambda_3 &= \tfrac{h}{H} = \lambda^{-2},\end{aligned} \tag{7}$$

where r, R and h, H are the current and referential radii and thicknesses of the sphere accordingly and the last equality in (7) is due to the incompressibility condition.

The corresponding principal values of the Cauchy stress are assumed in the form

$$\begin{aligned}\sigma_1 &= \sigma_2 = \sigma \\ \sigma_3 &= 0\end{aligned}. \tag{8}$$

The constitutive law (2) can then be written as follows

$$\sigma = 2\psi_1(\lambda^2 - \lambda^{-4}), \tag{9}$$

where $(8)_2$ has been used for finding the Lagrange multiplier.

To relate stretches to the internal pressure, p, we consider equilibrium of a half sphere

$$2\pi r h \sigma = \pi r^2 p, \tag{10}$$

Accounting for Eqs. (7)–(9) this equation takes the final form

$$p(\lambda) = \frac{4H}{\lambda R}(1 - \lambda^{-6})\psi_1, \tag{11}$$

where ψ_1 is defined in (3) and the first principal invariant is

$$I_1 = 2\lambda^2 + \lambda^{-4}. \tag{12}$$

Combining (3), (11), and (12) leads to a pressure–stretch curve, which is presented in Fig. 2, where the stable part is shown by the bold line and the peak pressure designates the onset of rupture. The dashed line corresponds to the unstable equilibrium of the failed AAA and it generally should be analyzed within the framework of elastodynamics concerning the failure propagation, which is beyond the scope of the present work.

3. Growth and remodeling

In order to include growth and remodeling in a mathematical description of the AAA evolution it is necessary to couple equations of the mass and momentum balance. The full-scale coupling should generally require the account of mass diffusion. However, we simplify the general model assuming that AAA is very thin and the mass supply is volumetric and homogeneous. Thus, we ignore the diffusion of mass. Under the mentioned assumption the mass balance equation reduces to the following evolution equation

$$\frac{\mathrm{d}}{\mathrm{d}t}\left(\frac{\rho(t)}{\rho_0}\right) = \left(a_1\left(\frac{\operatorname{tr}\boldsymbol{\sigma}(t)}{\operatorname{tr}\boldsymbol{\sigma}_0} - 1\right) + a_2\right)\frac{\rho(t)}{\rho_0}, \tag{13}$$

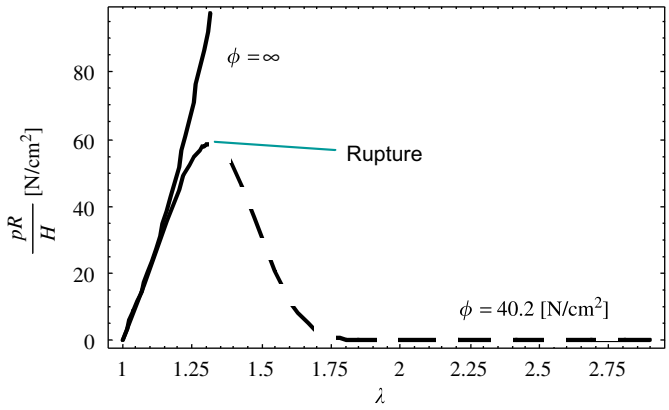

Fig. 2. Inflation and rupture of AAA balloon: bold and dashed lines designate stable and unstable branches of the curve accordingly. There is no rupture for the infinite average bond energy, $\phi = \infty$.

$$\frac{\rho(0)}{\rho_0} = 1 \tag{14}$$

where ρ is the referential mass density; $\rho_0 = \rho(0)$ is the initial mass density; a_1 is a constant of epigenetic growth—remodeling—and a_2 is a constant of the genetic growth; and $\boldsymbol{\sigma}_0 = \boldsymbol{\sigma}(t=0)$ is the Cauchy stress tensor at the onset of growth, $t = 0$.

Experiments have shown that AAA enlargement is accompanied by stiffening of the material on one hand,[1] and decreasing strength on the other hand: Lanne et al. (1992); MacSweeney et al. (1992); He and Roach (1994); Vorp et al. (1996a, b); Raghavan et al. (1996); Sonesson et al. (1997); Vorp et al. (2001); Di Martino et al. (2006); Vorp and Vande Geest (2005); Vande Geest et al. (2006). We mirror these material transformations by the following simple relationships

$$\frac{\alpha(t)}{\alpha_0} = \frac{\beta(t)}{\beta_0} = 1 + b_1\left(\frac{\rho(t)}{\rho_0} - 1\right)^{b_2}, \tag{15}$$

$$\frac{\phi(t)}{\phi_0} = \left(\frac{\alpha_0}{\alpha(t)}\right)^{b_3}, \tag{16}$$

where $\alpha_0 = \alpha(0)$, $\beta_0 = \beta(0)$, and $\phi_0 = \phi(0)$ are initial values of the material parameters at the onset of growth and b_1, b_2, and b_3 are the material constants.

Now, the evolving stored energy with account of growth takes the form

$$\psi(t) = \phi(t)\frac{\rho(t)}{\rho_0}\left[1 - \exp\left\{-\frac{\alpha(t)}{\phi(t)}(I_1(t)-3) - \frac{\beta(t)}{\phi(t)}(I_1(t)-3)^2 + \frac{\eta(\rho(t)-\rho_0)}{\phi(t)}(I_1(t)-3)\right\}\right], \tag{17}$$

where $\eta = \text{constant}$ is a growth modulus in the case of isotropic growth. Basically, the growth modulus is a product of an elastic modulus and the coefficient of the growth expansion—analogously to the coefficient of the thermal expansion in thermoelsticity. The discussion of the growth modulus and the analogy of growth with the thermal expansion can be found in Volokh (2004, 2006b).

It is of fundamental importance to realize that the process of growth (hours–months) occurs at a different time scale as compared to the process of deformation under mechanical loads (fractions of seconds). The latter means that there is no need, in our opinion, to *directly* couple both processes by introducing, for example, intermediate incompatible configurations of pure growth as it is often done in the literature.[2] Particularly, we assume that AAA can be described by the stored energy function (17) with the evolving material constants. The evolution of the material constants, (15) and (16), is controlled by the mass flow, (13) and (14), which is affected by the current stress state.

The pressure–stretch formula (11) should be adjusted accordingly

$$p(\lambda(t)) = \frac{4H}{\lambda(t)R}(1 - \lambda(t)^{-6})\psi_1(t), \tag{18}$$

where

$$\psi_1 = \frac{\rho(t)}{\rho_0}\{\alpha(t) - \eta(\rho(t)-\rho_0) + 2\beta(t)(I_1(t)-3)\} \times \exp\left\{-\frac{\alpha(t)}{\phi(t)}(I_1(t)-3) - \frac{\beta(t)}{\phi(t)}(I_1(t)-3)^2 + \frac{\eta(\rho(t)-\rho_0)}{\phi(t)}(I_1(t)-3)\right\}. \tag{19}$$

Fig. 3 presents various pressure–stretch curves for the evolving mass density with account of (15)–(19) and $b_1 = 100$; $b_2 = 1$; $b_3 = 3$; $\eta = 1300\,\text{N cm/kg}$; $\alpha_0 = 10.3\,\text{N/cm}^2$; $\beta_0 = 18.0\,\text{N/cm}^2$; and $\phi_0 = 40.2\,\text{N/cm}^2$.

Considering the specific problem of the growing AAA we have to solve the initial-value problem (13) and (14) under the imposed constraint (18).

The evolution Eq. (13) can be further transformed by introducing the dimensionless time, $\bar{t} = t/t^*$, where t^* is a characteristic time. In this case we have the following constrained initial-value problem:

$$\frac{\mathrm{d}}{\mathrm{d}\bar{t}}\left(\frac{\rho(\bar{t})}{\rho_0}\right) = \left(\bar{a}_1\left(\frac{\operatorname{tr}\boldsymbol{\sigma}(\bar{t})}{\operatorname{tr}\boldsymbol{\sigma}_0} - 1\right) + \bar{a}_2\right)\frac{\rho(\bar{t})}{\rho_0}, \quad \frac{\rho(0)}{\rho_0} = 1, \tag{20}$$

$$p = \frac{4H}{\lambda(\bar{t})R}(1 - \lambda(\bar{t})^{-6})\psi_1(\bar{t}) = \text{constant}, \tag{21}$$

where $\bar{a}_i = a_i t^*$ and the material parameters are changing in accordance with (15) and (16).

Finally, we should notice that the proposed model of growth is phenomenological and it accounts for the microstructural changes, such as the elastin degradation or collagen remodeling, through the changes of the macroscopic parameters, such as stiffness, strength, mass density, etc. We avoid a distinction between various

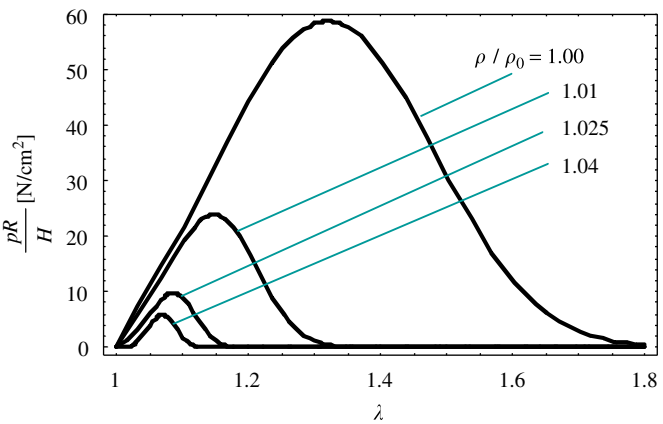

Fig. 3. Pressure–stretch curves for the evolving mass density.

[1] We should note, however, that results of Long et al. (2004) suggest that beyond the diameter 5 cm AAA can become compliant again.

[2] The multiplicative decomposition of the tensor of deformation gradient is often used to describe the pointwise configuration of 'pure growth'. The physical meaning of the decomposition and the intermediate growth configuration needs further clarification.

constituents because it can significantly complicate the model, which would be undesirable at the initial stages of the theory development.

4. Results

We use the numerical procedure 'NDSolve' of Mathematica 5.2 (Wolfram, 2003) for solving (20) and (21). This procedure allows solving a system of differential-algebraic equations based on the IDA package, which is a part of the software developed at the Center for Applied Scientific Computing of Lawrence Livermore National Laboratory. It solves the system of differential-algebraic equations by combining the Backward Differential Formula methods and Newton-type methods. The procedure provides the converging results as long as there is no failure in AAA tissue. After the point of rupture no solution of the constraint (21) exists and the numerical process does not converge. In other words, the point where the convergence fails is the point of the AAA rupture.

The points of rupture are starred in Fig. 4 where the simulations of the AAA evolution are shown for the constant internal pressure: $pR/H = 15\,\mathrm{N/cm^2}$ and the following values of the material constants: $\bar{a}_1 = 1$; $\bar{a}_2 = 10$; $b_1 = 100$; $b_2 = 1$; $b_3 = 3$; $\alpha_0 = 10.3\,\mathrm{N/cm^2}$; $\beta_0 = 18.0\,\mathrm{N/cm^2}$; and $\phi_0 = 40.2\,\mathrm{N/cm^2}$. Another set of simulations has been done for varying $\bar{a}_1 = 1$; 10; 100 and $\eta = 1300\,\mathrm{N\,cm/kg}$ and is presented in Fig. 5. The final set of simulations is given in Fig. 6 for varying b_1; $\bar{a}_1 = 10$; and $\eta = 1300\,\mathrm{N\,cm/kg}$. The considered sets of material parameters allow for the essential flexibility in the description of AAA growth and rupture.

We should emphasize that our choice of the material constants led to a relatively low stretch values at the point of rupture. The relatively low rupture stretch shows that a rational model can predict rupture of small aneurysms in

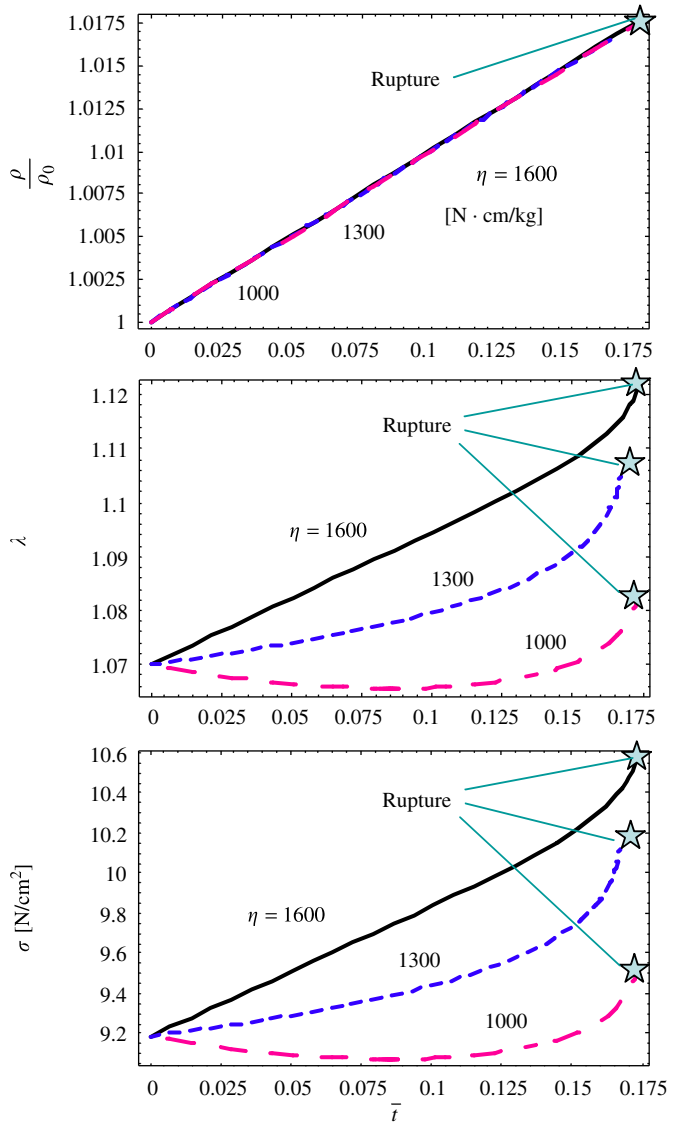

Fig. 4. Evolution of density, stretch and stress for the spherical AAA with varying η.

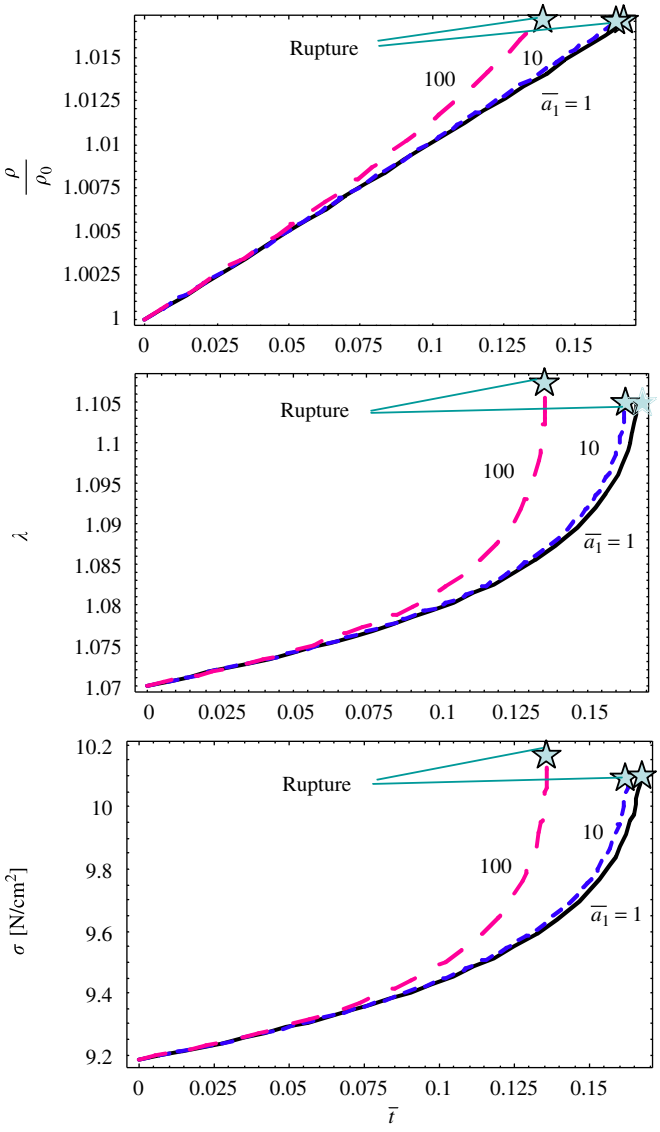

Fig. 5. Evolution of density, stretch and stress for the spherical AAA with varying $\bar{a}_1$.

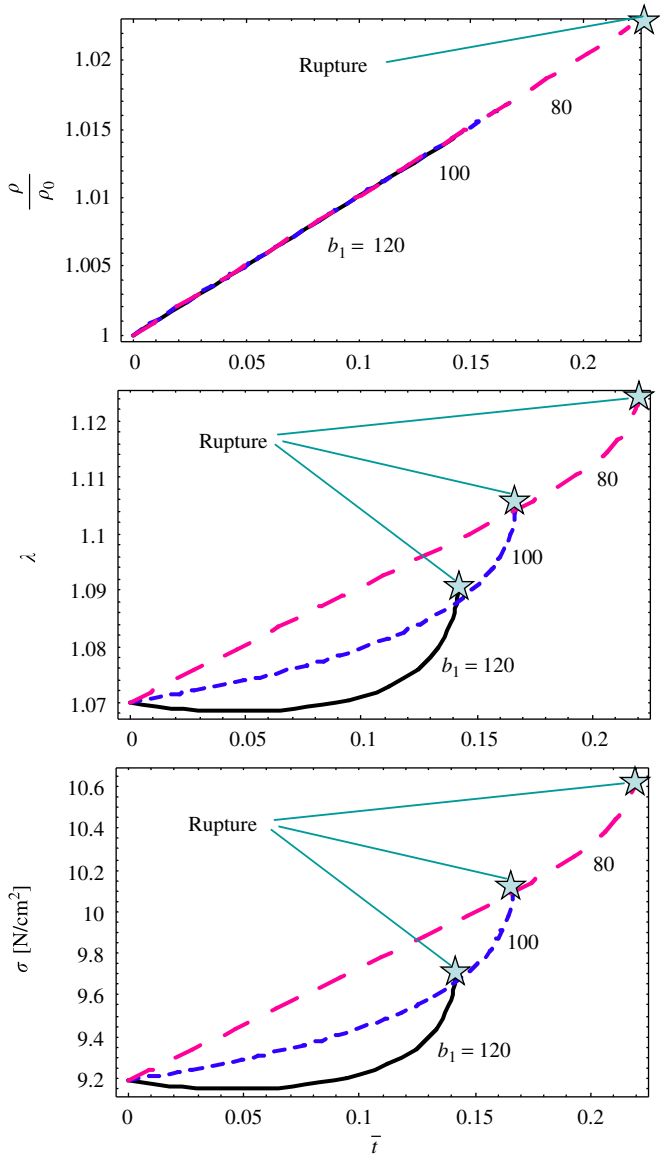

Fig. 6. Evolution of density, stretch and stress for the spherical AAA with varying b_1.

contrast to the traditional empirical criteria capturing rupture of big aneurysms predominantly. Of course, the considered sets of constants are arbitrarily chosen for the sake of the illustration of the model capabilities. The realistic calibration of the model will require experiments and clinical observations.

5. Discussion

We proposed a mathematical model describing growth and rupture of the AAA. This model includes equations of the momentum and mass balance and the constitutive law is enhanced with the influence of the mass change. The evolution of the material constants during growth is also taken into account. Failure is described by inducing the average bond energy limit, ϕ, in the stored energy function. Such a limit controls material softening indicating failure. The initial values of the AAA material constants including failure (α, β, ϕ) were calibrated in the uniaxial tension test. The description of AAA growth is based on the assumption that the mass supply and turnover should be accompanied by the change of mass density. Such a change is visible in hard tissues; for example, the cancellous bone has a stiff microstructure whose evolution in growth is accompanied by a pronounced density alteration (Cowin, 2001). Soft tissues do not enjoy a stiff microstructure like bone. The change of the mass density in soft tissues is less pronounced and its observation is more complicated. Nonetheless, there is no physical reason, in our opinion, to expect that the growth process is fundamentally different in hard and soft tissues.

Based on the proposed model, we considered growth and rupture of an idealized spherical AAA. The results of analysis are reasonable qualitatively though the quantitative calibration of the model will require further clinical observations and in vitro tests. The proposed set of material constants is relatively large: a_1; a_2; b_1; b_2; b_3; and η. The latter was done intentionally because it would allow for more flexibility in fitting experiments. Ideally, one should be able to follow up the mass flow and shape and structure change of the growing AAA until rupture. Though we believe that noninvasive techniques will allow such observations in the future, more realistically, calibration of the model should be implicit and based on the observation of the evolution of the AAA shape.

Concerning limitations of the present work we should note first of all that the considered example of AAA is highly idealized—it is a thin spherical shell under radial inflation. Our choice was driven by the desire to have simple (semi-) analytically tractable solutions. More sophisticated shapes are required for modeling realistic aneurysms. Such shapes will require the spatial finite element discretizations (see Baek et al., 2006, for example). Nonetheless, we should emphasize that the goal of the present work was not to model a specific AAA, but rather to develop a mathematical framework suitable for simulating the aneurysm enlargement and rupture. The latter, i.e. coupling of growth and rupture, is essentially novel and has not been considered in the literature previously.

Conflict of interest

None declared.

References

Baek, S., Rajagopal, K.R., Humphrey, J.D., 2006. A theoretical model of enlarging intracranial fusiform aneurysms. Journal of Biomechanical Engineering 128, 142–149.

Bengtsson, H., Sonesson, B., Bergqvist, D., 1996. Incidence and prevalence of abdominal aortic aneurysms, estimated by necropsy studies and population screening by ultrasound. Annals of the New York Academy of Sciences 800, 1–24.

Cowin, S.C. (Ed.), 2001. Bone Mechanics Handbook. CRC Press, Boca Raton.

Di Martino, E., Bohra, A., Vande Geest, J., Gupta, N., Makaroun, M., Vorp, D., 2006. Biomechanical properties of ruptured versus non-ruptured abdominal aortic aneurysm wall tissue. Journal of Vascular Surgery 43, 570–576.

Elger, D.F., Blackketter, D.M., Budwig, R.S., Johansen, K.H., 1996. The influence of shape on the stresses in model abdominal aortic aneurysms. Journal of Biomechanical Engineering 118, 326–332.

He, C.M., Roach, M.R., 1994. The composition and mechanical properties of abdominal aortic aneurysms. Journal of Vascular Surgery 21, 6–13.

Humphrey, J.D., Canham, P.B., 2000. Structure, mechanical properties, and mechanics of intracranial saccular aneurysms. Journal of Elasticity 61, 49–81.

Lanne, T., Sonesson, B., Bergqvist, D., Bengtsson, H., Gustafsson, D., 1992. Diameter and compliance in the male human abdominal aorta: influence of age and aortic aneurysm. European Journal of Vascular Surgery 6, 178–184.

Li, Z., Kleinstreuer, C., 2005. A new wall stress equation for aneurysm rupture prediction. Annals of Biomedical Engineering 33, 209–213.

Long, A., Rouet, L., Bissery, A., Rossignol, P., Mouradian, D., Sapoval, M., 2004. Compliance of abdominal aortic aneurysms: evaluation of tissue Doppler imaging. Ultrasound in Medicine & Biology 30, 1099–1108.

MacSweeney, S.T., Young, G., Greenhalgh, R.M., Powell, J.T., 1992. Mechanical properties of the aneurysmal aorta. British Journal of Surgery 79, 1281–1284.

Ouriel, K., Green, R.M., Donayre, C., Shortell, C.K., Elliott, J., DeWeese, J.A., 1992. An evaluation of new methods of expressing aortic aneurysm size: relationship to rupture. Journal of Vascular Surgery 15, 12–20.

Patel, M.I., Hardman, D.T., Fisher, C.M., Appleberg, M., 1995. Current views on the pathogenesis of abdominal aortic aneurysms. Journal of American College of Surgery 181, 371–382.

Raghavan, M.L., Vorp, D.A., 2000. Toward a biomechanical tool to evaluate rupture potential of abdominal aortic aneurysm: identification of a finite strain constitutive model and evaluation of its applicability. Journal of Biomechanics 33, 475–482.

Raghavan, M.L., Webster, M.W., Vorp, D.A., 1996. Ex-vivo biomechanical behavior of abdominal aortic aneurysm: assessment using a new mathematical model. Annals of Biomedical Engineering 24, 573–582.

Sonesson, B., Hansen, F., Lanne, T., 1997. Abdominal aortic aneurysm: a general defect in the vasculature with focal manifestations in the abdominal aorta? Journal of Vascular Surgery 26, 247–254.

Vande Geest, J.P., Sacks, M.S., Vorp, D.A., 2006. The effect of the aneurysm on the biaxial mechanical behavior of human abdominal aorta. Journal of Biomechanics 39, 1324–1334.

Volokh, K.Y., 2004. A simple phenomenological theory of tissue growth. Mechanics and Chemistry of Biosystems 1, 147–160.

Volokh, K.Y., 2006a. Compressibility of arterial wall in ring-cutting experiments. Molecular and Cellular Biomechanics 3, 35–42.

Volokh, K.Y., 2006b. Stresses in growing soft tissues. Acta Biomaterialia 2, 493–504.

Volokh, K.Y., 2007. Hyperelasticity with softening for modeling materials failure. Journal of the Mechanics and Physics of Solids 55, 2237–2264.

Volokh, K.Y., 2008. Prediction of arterial failure based on a micro-structural bi-layer fiber-matrix model with softening. Journal of Biomechanics 41, 447–453.

Vorp, D.A., 2007. Biomechanics of abdominal aortic aneurysm. Journal of Biomechanics 40, 1887–1902.

Vorp, D.A., Vande Geest, J.P., 2005. Arteriosclerosis Thrombosis and Vascular Biology 25, 1558–1566.

Vorp, D.A., Mandarino, W.A., Webster, M.W., Gorcsan, J., 1996a. Potential influence of intraluminal thrombus on abdominal aortic aneurysm as assessed by a new non-invasive method. Cardiovascular Surgery 4, 732–739.

Vorp, D.A., Raghavan, M.L., Muluk, S.C., Makaroun, M.S., Steed, D.L., Shapiro, R., Webster, M.W., 1996b. Wall strength and stiffness of aneurysmal and nonaneurysmal abdominal aorta. Annals of the New York Academy of Sciences 800, 274–276.

Vorp, D.A., Lee, P.C., Wang, D.H.J., Makaroun, M.S., Nemoto, E.M., Ogawa, S., Webster, M.W., 2001. Association of intraluminal thrombus in abdominal aortic aneurysm with local hypoxia and wall weakening. Journal of Vascular Surgery 34, 291–299.

Watton, P.N., Hill, N.A., Heil, M., 2004. A mathematical model for the growth of the abdominal aortic aneurysm. Biomechanics and Modeling in Mechanobiology 3, 98–113.

Wolfram, S., 2003. The Mathematica Book, fifth ed.. Wolfram Media.